

Myocardial signal intensity decay after gadolinium injection: a fast and effective method for the diagnosis of cardiac amyloidosis

Giovanni Donato Aquaro · Nicola Riccardo Pugliese · Federico Perfetto · Francesco Cappelli · Andrea Barison · Pier Giorgio Masci · Claudio Passino · Michele Emdin

Received: 30 January 2014 / Accepted: 26 April 2014 / Published online: 1 May 2014
© Springer Science+Business Media Dordrecht 2014

Abstract Late Gadolinium Enhancement (LGE) pattern of cardiac amyloidosis (CA) at cardiac magnetic resonance (CMR) examination is absent in approximately 30 % of patients. We tested whether the evaluation of myocardial gadolinium signal intensity (SI) decay (SID) has a higher diagnostic accuracy for CA. CMR was performed in 59 patients with systemic AL amyloidosis (36 males, 69 ± 10 years, mean \pm SD), and 20 age/sex-matched healthy controls. LGE images were acquired every minute up to 8 min after gadolinium injection (time of inversion 250 ms). SI regions of interest were plotted in SI/time curves for endocardial (Endo) and epicardial layer of interventricular septum, cavity, and skeletal muscle as reference. SID (a negative exponential function described by the parameter T_{SID}) was expressed as number of heart beats (HB) from each ROI. The typical LGE pattern for CA was detected in 42 patients (Ty-LGE), while 17 showed either absent LGE or an atypical pattern (ATy-LGE). A definite CA diagnosis was confirmed in all Ty-LGE patients and in 10/17 ATy-LGE patients. At ROC analysis Endo- T_{SID} was the most accurate parameter to distinguish Ty-LGE and ATy-LGE patients from controls. A 269 HB threshold (mean + 2 SD Endo- T_{SID} measured in controls) identified 51/52 patients with definite CA diagnosis, with 98 % sensitivity, 93 % specificity, and 96 % diagnostic

accuracy. A direct relation was found between the extracellular volume and Endo- T_{SID} in CA patients (r 0.72, 95 % CI 0.37–0.89, $p < 0.001$). the analysis of myocardial SID after gadolinium injection improves the accuracy of CMR for CA diagnosis.

Keywords Cardiac amyloidosis · Cardiac magnetic resonance · Late gadolinium enhancement

Abbreviations

AL	Amyloid light chain
ARB	Angiotensin receptor blocker
BMI	Body mass index
CA	Cardiac amyloidosis
CKD	Chronic kidney disease
CMR	Cardiac magnetic resonance
COPD	Chronic obstructive pulmonary disease
EGFR	Estimated glomerular filtration rate
LGE	Late gadolinium enhancement
MGUS	Monoclonal gammopathy of undetermined significance
NYHA	New York Heart Association
ROI	Region of interest
SD	Standard deviation
SID	Signal intensity decay

G. D. Aquaro (✉) · P. G. Masci · M. Emdin
Fondazione G. Monasterio CNR-Regione Toscana, Via Moruzzi,
1, 56124 Pisa, Italy
e-mail: aquaro@ftgm.it

N. R. Pugliese · A. Barison · C. Passino · M. Emdin
Cardio-Thoracic and Vascular Department, Pisa, Italy

F. Perfetto · F. Cappelli
Regional Amyloid Center, AOU Careggi Firenze, Florence, Italy

Introduction

Cardiac involvement is a frequent cause of death in patients with AL (amyloid light chain) amyloidosis [1]. A combination of clinical, electrocardiographic and imaging methods is commonly used to diagnose cardiac amyloidosis (CA) in patients with systemic amyloidosis, by the

evidence of concentric left ventricular (LV) hypertrophy by echocardiography, combined with electrocardiogram (ECG) low voltage QRS potentials, and positive noncardiac and cardiac biopsies [2]. However, echocardiography lacks of specificity (concentric hypertrophy being potentially secondary to other causes), ECG abnormalities may be absent in a percentage of CA patients, and endomyocardial biopsy is invasive, expensive and risky [2, 3].

Cardiovascular magnetic resonance (CMR) is an emerging imaging tool for the CA diagnosis [4, 5]. CMR allows identification of the morphological features of cardiac amyloidosis (concentric pseudohypertrophy, thickening of atrial walls), and may evidence, after gadolinium injection, cardiac amyloid involvement. The amyloid deposit increases the extracellular volume, and alters the myocardial wash-out of gadolinium [6], inducing a specific pattern at Late Gadolinium Enhancement (LGE) in CA patients, represented by a diffuse subendocardial and subepicardial (in advanced disease) enhancement, together with early darkening of cardiac chambers [6]. This LGE pattern has, however, a low sensitivity, being present only in 2/3 of CA patients [4], while the diagnostic accuracy of alternative CMR techniques, such as T1 mapping, is still under investigation [7–11].

Our hypothesis was that: (a) gadolinium kinetics might be evaluated by the analysis of myocardial Signal Intensity Decay (SID); (b) that the myocardial amyloid deposit could slow SID; (c) SID analysis could offer a quantitative approach to the early diagnosis of CA by CMR.

Aim of this study was then to test this hypothesis in CA patients with a preexisting diagnosis of systemic AL amyloidosis, and to compare the diagnostic accuracy of SID with LGE technique.

Methods

We enrolled 59 consecutive patients (36 males, age 69 ± 10 years, mean \pm SD), with a previous diagnosis of systemic AL amyloidosis and 20 healthy control subjects (12 males, age 65 ± 14 years). Monoclonal expansion and final diagnosis of multiple myeloma or monoclonal gammopathy of undetermined significance (MGUS) was confirmed by osteo-medullary biopsy. Abnormal proteins were detected in the bloodstream: we assessed the presence of κ - and λ -free light chains and κ/λ ratio on protein electrophoresis and immunofixation. Systemic AL amyloidosis was confirmed by periumbilical biopsy.

A complete clinical evaluation was performed at the enrollment. Presence and the severity of dyspnea was classified by New York Heart Association (NYHA) functional class. All enrolled patients had a thorough clinical, biohumoral, electrocardiographic and echocardiographic

evaluation before the enrollment. Biomarkers included serum creatinine, troponine I assay (evaluated by a chemiluminescent immunoassay, ADVIA cTnI-Ultra method, Siemens Medical Solutions, Erlangen, Germany) and plasma NT-proBNP assay (by Elecsys electrochemiluminescence method, Roche Diagnostics, Basel, Switzerland). Patients with contraindications for CMR and those with an estimated glomerular filtration rate (eGFR) <30 ml/min, by Cockcroft Gault formula were excluded from the study.

Diagnosis of CA was performed by the presence of echocardiographic criteria (LV wall thickness >12 mm or right ventricular—RV-free wall thickening coexisting with LV thickening in the absence of any other known cause) and/or electrocardiographic criteria (low potential QRS complex voltage) [2]. In case of absence of these echocardiographic and electrocardiographic criteria, we performed myocardial biopsy (Congo-red staining combined with polarized light). The study was approved by the institutional ethical committee, and all subjects gave their written informed consent.

CMR protocol

CMR was performed with a dedicated 1.5-T (Signa Hdx, General Electric Healthcare, Milwaukee, Wisconsin) with an 8-channel cardiac phased array coil. Short-axis cine images from the mitral plane valve to the LV apex were acquired using a steady-state free precessing FIESTA (fast imaging employing steady-state acquisition) pulse sequence with the following parameters: 30 phases, slice thickness 8 mm, no gap, 8 views per segment, number of excitation 1, field of view 40 cm, phase field of view 1, 224×224 matrix, voxel dimensions $1.78 \times 1.78 \times 8$ mm, reconstruction matrix 256×256 , 45° flip angle, repetition time/echo time equal to 3.5/1.5, and a bandwidth of 125 kHz. After cine imaging, 0.2 mmol/kg Gd-DTPA (Magnevist, Schering-AG, Berlin-Wedding, Germany) were injected in peripheral vein.

For the evaluation of SID technique LGE images were acquired in horizontal long axis view every minutes after the injection of Gd-DTPA for 8 consecutive minutes (Fig. 1). An inversion recovery gradient echo (GRE-IR) T1-weighted sequence was used with the following parameters: inversion time of 250 ms, field of view 40 mm, slice thickness 8 mm, no gap between each slice, repetition time 4.6 ms, echo time 1.3, 20° flip angle, matrix 224×224 , reconstruction matrix 256×256 , number of excitation 1.

Measurement of myocardial T1 was obtained using the MCine-IR sequence acquired in a same horizontal long axis view view before and at fixed time intervals (10 and 15 min) after the administration of gadolinium contrast

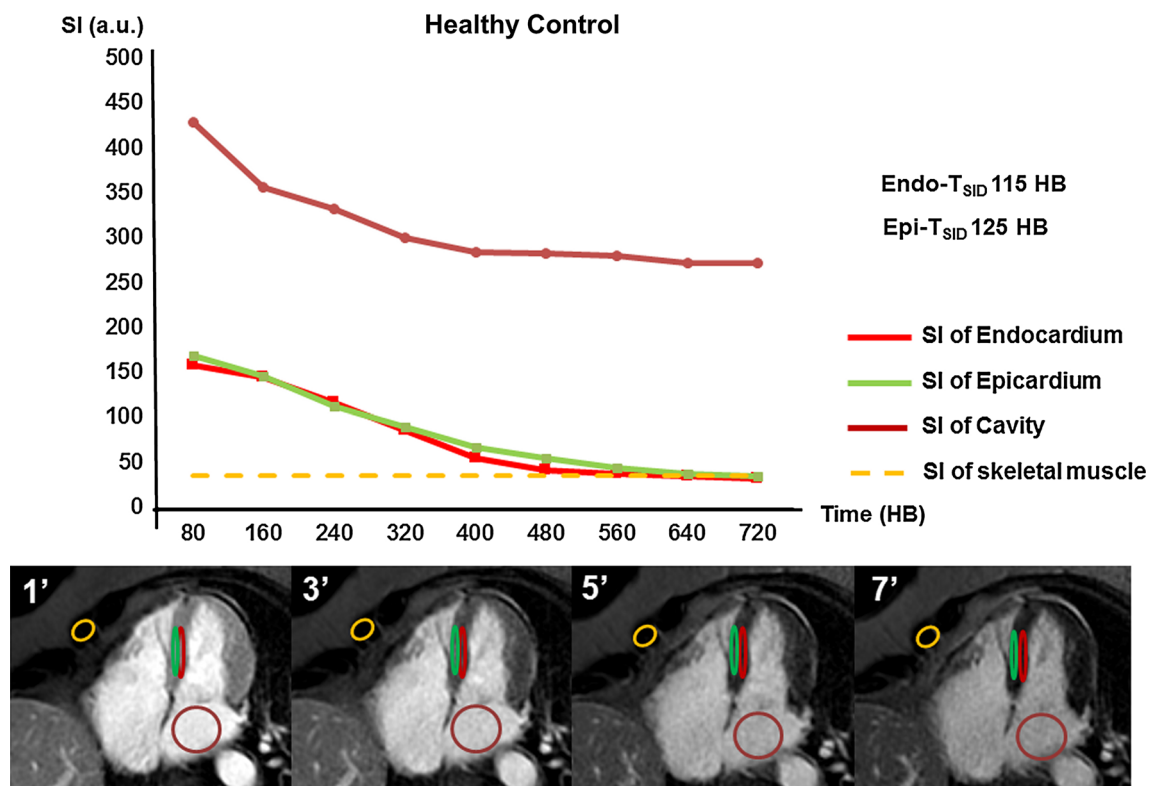


Fig. 1 Example of Signal Intensity Decay (SID) post gadolinium injection in a healthy patients. In the lower four panels are showed LGE images acquired with TI of 250 ms at 1, 3, 5 and 7 min after contrast injection. Regions of interest (ROI) are placed in the skeletal muscle (*orange*), in cavity (*brown*), and in endocardial (*red*) and epicardial (*green*) layers of interventricular septum. The average

signal intensity from each ROI is plotted against time (expressed as heart beats, HB) in the graph in the upper panel. In this case of a healthy patient, signal of endocardial and epicardial ROIs reached the signal of skeletal muscle, considered as referral, few minutes after injection

agents [12]. The following parameters were used for MCine-IR acquisition: field of view 38×38 cm, matrix 224×160 , flip angle 8° , echo time 2.4 ms, repetition time 5 ms, number of excitation 0.5 with 16 overscans.

Then, conventionally LGE images were acquired 10 min after the administration of the contrast medium in a full set of short-axis views in the same plane of cine images. An inversion recovery T1-weighted gradient echo sequence was used with the same parameters as for SID but with a variable inversion time trying to null normal myocardium. In CA, it is often difficult to determine the optimal inversion time to null myocardium.

Image analysis

Analysis of CMR images was performed, using a commercially available research software package (Mass Analysis 6.1, Leiden, the Netherlands). LV and right ventricle RV mass was measured by the analysis of the cine short-axis LGE images. The endocardial and epicardial (Epi) contours of LV and RV myocardium were manually traced in the end-diastolic and the end-systolic phases.

End-diastolic volume index, end-systolic volume index, mass and mass index were measured as previously described [13–15]. The LV and RV volumetric data were plotted against the time (in ms) in a volumetric filling time curve. LV diastolic parameters were calculated from the volumes/time curve as previously described [16]. Briefly, a dV/dT curve was generated as the first-derivative transformation of the volumetric filling time curve. The early (E) and late (A) peak filling rate (PFR) were measured in dV/dT curve as, respectively, the early and the late diastolic peaks of dV/dT curve. The PFR_E/PFR_A ratio was defined as the ratio between the early and the late peak filling rates.

The analysis of SID was performed with FuncTool software (General Electric Healthcare[®], 2008). Briefly, in each image regions of interest (ROIs) were manually traced to quantify the SI in the following cardiac areas: (1) endocardium of interventricular septum, (2) subepicardium of interventricular septum, (3) left atrium cavity (to assess signal intensity within cardiac chambers), (4) a skeletal muscle of the anterior chest wall as close as possible to the heart. The skeletal muscle ROI was chosen as an ideal

reference area. In fact in resting condition, in absence of hyperemia, blood flow of skeletal muscle is decreased showing only a minimal enhancement immediately after contrast injection. Then signal intensity of skeletal muscle is nulled few minutes after contrast medium injection and it has the same inversion time of the normal myocardium.

Signal intensity was automatically measured for each ROI generating myocardial SI/time curves. Because the wash-out kinetic of gadolinium may be influenced by different hemodynamics conditions, as different heart rate, the time variable was expressed in heartbeats (HB) to provide uniform and comparable SI/time curves and to minimize the gadolinium washout differences.

In agreement with previous evidences evaluation of myocardial SID after Gd-DTPA injection has been realized as follows [17]. The SID may be modeled as a negative exponential decay equation:

$$S_i = C_{sm} + S_0 x \frac{-T_i}{e^{T_{SID}}} \quad (1)$$

where S_i is the myocardial signal intensity at time T_i ; C_{sm} is the average signal intensity of skeletal muscle and represents the theoretical value toward which tends the myocardial signal during the wash-out of gadolinium; T_{SID} is the time-constant describing the signal decay; S_0 is y-intercept of signal intensity representing the initial myocardial signal intensity. Equation 1 was numerically solved by minimizing the mean square error in Matlab software by using the Levenberg–Marquardt method. The average normalized mean square error between measured signal intensity/time curve and equation, expressed as percentage, was $<5\%$ demonstrating the effectiveness of the assumption.

Defining T_n as the time of myocardial signal intensity to reach C_{sm} (with $T_n \gg T_{SID}$), when $T_i = T_n$ the following equation is obtained:

$$T_n = T_{SID} x \ln \frac{S_i - C_{sm}}{S_0} \quad (2)$$

As demonstrated by this equation, T_{SID} was the parameter permitting to evaluate SID.

The analysis of conventional LGE images was performed by 3 expert investigators ($>1,000$ CMR examination), blinded of the clinical history of the patients, who independently evaluated the presence or absence of the typical LGE pattern of CA, represented by diffuse subendocardial hyperenhancement and early darkening of signal of ventricular cavity [18]. Then, population was subdivided in three groups based on LGE findings: (1) patients with CA and the typical LGE pattern (Ty-LGE); (2) patients with area of myocardial enhancement at LGE images but without the typical pattern of LGE or even without myocardial enhancement (ATy-LGE); (3) healthy control subjects.

The volume of distribution of gadolinium in myocardium, also defined as extracellular volume (ECV) was measured as previously described [19]. Briefly, The volume of distribution in the myocardium, also known as the extracellular volume, ECV, is then calculated as:

$$ECV = (1 - \text{Hematocrit}) \times (\Delta R1_{\text{myocardium}} / \Delta R1_{\text{blood}})$$

where $\Delta R1$ is $(1/T1 \text{ post contrast} - 1/T1 \text{ pre contrast})$. Myocardial $T1$ measurements was performed in the intraventricular septum and it was obtained as previously reported [12].

Statistical analysis

Continuous values are expressed as the mean \pm standard deviation for normally distributed variables and as median (25th to 75th percentile) for variables with non-normal distributions. Variables with skewed distributions were logarithmically transformed before further analysis. Categorical variables were compared by Pearson's Chi square test or Fisher's exact test, when appropriate. One-way analysis of variance or Bonferroni's post hoc test, when appropriate, was used to compare quantitative variables across groups. A p value < 0.05 was considered statistically significant. Receiver operating characteristic curves were used to evaluate the specificity and sensitivity of parameters of myocardial SID (Endo- T_{SID} , Epi- T_{SID}) to discriminate Ty-LGE, ATy-LGE, No-LGE and Control groups.

Results

Characteristics of population are showed in Table 1. Forty-one patients with systemic AL amyloidosis (69 %) were affected by multiple myeloma, and 18 patients (31 %) by MGUS. Fifty-one patients (86 %) had dyspnea (NYHA class II: 48 %; III: 30 %; IV: 8 %). The median NT-proBNP plasma level was 6,437 ng/L (2,305–14,465). A reduced kidney function (chronic kidney disease stage 3, $30 \text{ mL/min} < \text{eGFR} < 60 \text{ mL/min}$) was observed in 30 patients (51 %). Immunoglobulin light chains were increased in 30 patients (51 %); free light chains (FLCs) were increased with the inversion of κ/λ ratio in 87 % of patients (λ -FLCs median: 47, 23–119; κ/λ ratio median 0.06, 0.02–0.62). All patients with active myeloma underwent a specific therapy with a scheme of drug association. Cardiovascular therapy was reported in Table 1. Endomyocardial biopsy was performed in 8 patients (14 %) with no echocardiographic and electrocardiographic criteria. Finally, a definite diagnosis of CA was obtained in 52 patients (88 %) with systemic AL amyloidosis.

Table 1 Characteristics of the patient population

Variables	Data
General characteristics:	
Age (years)	69 ± 10
Males n(%)	36 (61)
Multiple myeloma, n (%)	41 (69)
MGUS, n (%)	18 (31)
BMI (kg/m ²)	25.3 ± 4
Diabetes mellitus, n (%)	13 (22)
Arterial hypertension, n (%)	35 (59)
Dyslipidemia, n (%)	18 (31)
Smoke, n (%)	21 (36)
History of cardiovascular disease	21 (36)
Atrial fibrillation, n (%)	20 (34)
COPD, n (%)	12 (20)
Renal function	
Serum creatinine (mg/dL)	1.6 ± 1
eGFR (mL/min)	59.2 ± 32
CKD stages	
1, n (%)	13 (22)
2, n (%)	16 (27)
3, n (%)	30 (51)
NYHA class	
I, n (%)	8 (14)
II, n (%)	28 (48)
III, n(%)	18 (30)
IV, n (%)	5 (8)
Biomarkers:	
Troponine I (ng/mL)	0.36 ± 0.2
NT-proBNP (ng/L)	6,437 (2,305–14,465)
Echocardiogram:	
Ejection fraction (%)	58 ± 12
Septal thickness (mm)	15.1 ± 4
E/A	1.3 ± 1
E/E'	17.8 ± 7
Diagnosis of Systemic Amyloidosis by:	
Periumbilical biopsy, n (%)	40 (68)
Bone marrow biopsy, n (%)	38 (64)
Endomyocardial biopsy, n (%)	8 (14)
Immunoglobulin light chain:	
κ (mg/dL)	164 (123–285)
λ (mg/dL)	183 (105–376)
κ/λ	1.38 (0.37–1.8)
Immunoglobulin free light chain:	
κ (mg/dL)	6 (1.7–17.6)
λ (mg/dL)	47 (23–119)
κ/λ	0.06 (0.02–0.62)
Therapy:	
Specific therapy*, n (%)	28 (48)
Cardiac therapy, n (%)	53 (90)

Table 1 continued

Variables	Data
β-blockers, n (%)	35 (59)
ACE inhibitors or ARBs, n (%)	30 (51)
Diuretics, n (%)	45 (76)

Values are expressed as mean ± SD for continuous normally distributed variables and as median (25th to 75th percentile) for continuous non-normally distributed variables, unless otherwise stated

BMI body mass index, *COPD* chronic obstructive pulmonary disease, *EGFR* estimated glomerula filtratration rate, *CKD* chronic kidney disease, *NYHA* New York Heart Association, *ARB* angiotensin receptor blocker

CMR: morphological and functional characteristics

Morphological and functional characteristics of the groups are reported in Table 2. By the visual analysis of the conventional LGE images, patients were divided in 2 groups, accordingly to the pattern of LGE: 42 (70 %) were included in the Ty-LGE group; 17 patients (30 %) were in the ATy-LGE group: 4 (7 %) with myocardial areas with a LGE distribution different from the typical one, and 13 (23 %) with no LGE. A perfect matching between the investigators were recorded for the visual assessment of the LGE.

The end-diastolic wall thickness measured either in interventricular septum or inferolateral wall was higher in Ty-LGE than in ATy-LGE group, and in this latter subset than in controls (Table 2). LV mass index was higher in Ty-LGE than other groups and in ATy-LGE than controls, with a pattern of symmetrical pseudohypertrophy in both Ty-LGE and ATy-LGE subsets.

Ty-LGE patients showed a slight reduction in LV ejection fraction, as compared to controls while no difference was found for ATy-LGE. The average wall motion score index, not significantly different between Ty-LGE and ATy-LGE, but was higher in both subsets with amyloidosis than in controls.

Diastolic function was significantly compromised in all patients. The average left atrial area was higher in patients than controls, with no significant difference between Ty-LGE and ATy-LGE groups. Accordingly to referral values, 25 (60 %) patients in Ty-LGE group and 6 (33 %) in ATy-LGE groups had left atrial dilatation [17]. The prevalence of thickened interatrial septum, defined as thickness >5 mm in absence of septal lipomatosis, was no significantly different in Ty-LGE group, when compared to ATy-LGE group (57 vs. 33 %, $p = 0.07$).

Pericardial effusion was higher in Ty-LGE than in ATy-LGE group (54 vs. 11 %, $p = 0.005$), with a similar, non-significant prevalence for pleural effusion (54 vs. 24 %, $p = 0.07$).

Table 2 CMR: morphologic parameters

	Ty-LGE	<i>P</i> value*	ATy-LGE	<i>P</i> value**	Controls	<i>P</i> value***
Patients, n	42		17		20	
Males n (%)	30 (71)	0.5	11 (61)	0.5	15 (75)	0.9
Age (years)	71 ± 11	0.08	65 ± 8	0.5	65 ± 14	0.08
Left ventricle:						
IV Septal Thickness (mm)	19.2 ± 5	<0.001	13.7 ± 3	<0.001	8.9 ± 2	<0.001
Inf-lat thickness (mm)	14.1 ± 3	<0.001	9.8 ± 2	0.004	7.8 ± 2	<0.001
WMSI	1.4 ± 0.5	0.9	1.4 ± 0.6	0.007	1	0.002
LV EDVi (mL/m ²)	70.7 ± 23	0.01	90.4 ± 34	0.1	77.1 ± 17	0.3
LV ESVi (mL/m ²)	33.3 ± 17	0.06	45.3 ± 33	0.07	28.5 ± 8	0.3
LV EF (%)	53.8 ± 11	0.7	55.3 ± 19	0.1	62.4 ± 5	0.008
LV Mi (g/m ²)	119.8 ± 42	0.02	91.7 ± 34	0.09	75 ± 11	<0.001
LV Mi/VTDi	1.8 ± 0.6	<0.001	1.1 ± 0.3	0.6	1.1 ± 0.3	<0.001
Diastolic function:						
PFR _E	288.5 ± 134	0.8	281.5 ± 146	0.03	388 ± 140	<0.01
PFR _A	147.9 ± 161	0.04	242.9 ± 145	<0.001	441 ± 82	<0.001
PFR _E /PFR _A	3 ± 2.5	0.05	1.7 ± 1.6	0.02	0.8 ± 0.34	<0.001
Right ventricle:						
RV EDVi (mL/m ²)	64.6 ± 20	0.5	68.2 ± 20	0.1	84.4 ± 34	0.01
RV ESVi (mL/m ²)	29.4 ± 13	0.4	26.5 ± 13	0.2	31.3 ± 12	0.6
RV EF (%)	54.9 ± 12	0.09	60.9 ± 11	0.8	61.8 ± 6	0.05
Atria:						
Left atrial area (cm ² /m ²)	16.3 ± 4	0.1	14.6 ± 5	0.1	12.2 ± 2	<0.001
Right atrial area (cm ² /m ²)	13.8 ± 3	0.1	12.2 ± 2	0.3	11.1 ± 2	0.009
Thickened IA septum n (%)	24 (56)	0.2	6 (35)	0.01	0	<0.001
Pericardial effusion, n (%)	23 (54)	0.005	2 (12)	0.2	0	<0.001
Pleural effusion, n (%)	23 (54)	0.07	4 (24)	0.08	0	<0.001

* Ty-LGE versus ATy-LGE;
 ** ATy-LGE versus Healthy controls;

*** Ty-LGE versus Healthy controls

Ty-LGE typical LGE pattern, ATy-LGE non typical pattern or absence of LGE, LV left ventricle, EDVi end-diastolic volume index, ESVi end-systolic volume index, IV interventricular, Mi mass index, EF ejection fraction, WMSI wall motion score index, PFR peak filling rate, IA interatrial (thickened: IA septum > 5 mm), RV right ventricle

A definite diagnosis of CA was established in all Ty-LGE patients, and in 10 (59 %) of ATy-LGE patients (4/4 patients with atypical myocardial enhancement, and 6/13 with absence of myocardial enhancement).

Dynamics of signal intensity decay at CMR

Parameters of SID were reported in Table 3. The signal intensity of both endocardial and epicardial layers of interventricular septum at time 0 (Endo-S₀ and Epi-S₀, respectively) was not significantly different among Ty-LGE, ATy-LGE and controls. Examples of SID analysis are shown in CA patients in Figs. 2 and 3.

Parameters of SID (T_{SID} and T_n) measured at both endocardium and epicardium level were significantly higher in Ty-LGE than in ATy-LGE and in controls. The same parameters were also higher in ATy-LGE than in controls.

The comparison of ROC curves showed that Endo-T_{SID} was more accurate than Epi-T_{SID} for the distinction between patients with CA and controls (AUC 0.98, 95 % CI 0.93–0.99 vs. AUC 0.92, 95 % CI 0.83–0.96, *p* < 0.01). Endo-T_{SID} with a threshold value >272 HB allowed a full distinction between Ty-LGE and controls (AUC 1).

Moreover, Endo-T_{SID} was the most accurate for differentiating patients with ATy-LGE and obtaining a definite diagnosis of CA (AUC 0.95), with respect to the control subset, with a sensitivity of 90 % and a specificity of 94 % (Cut-point > 265 HB) (Fig. 4). Finally, Endo-T_{SID} with (cut-point > 272 HB) demonstrated a sensitivity of 96 % and specificity of 96 % to distinguish the whole population of patients with CA amyloidosis from healthy controls (AUC 0.98) (Fig. 4).

The Endo-T_n and Epi-T_n parameters were significantly higher in Ty-LGE than ATy-LGE and in this latter subset than controls.

Table 3 Signal intensity decay (SID): parameters analysis

SID parameters	Ty-LGE	<i>P</i> *	ATy-LGE	<i>P</i> **	Healthy controls	<i>P</i> ***
Heart Rate (bpm)	70 ± 12	0.5	72 ± 13	0.1	65.5 ± 12	0.2
<i>C</i> _{sm} (a.u.)	32 ± 6	0.08	28 ± 9	0.4	26 ± 5	0.001
Endo- <i>S</i> ₀ (a.u.)	170 ± 87	0.69	160 ± 92	0.50	181 ± 60	0.76
Endo- <i>T</i> _{SID} (HB)	1,142 ± 713	<0.001	365 ± 224	<0.001	175 ± 47	<0.001
Endo- <i>T</i> _n (HB)	4,447 ± 2,722	<0.001	1,395 ± 775	<0.001	738 ± 195	<0.001
Epi- <i>S</i> ₀ (a.u.)	164 ± 82	0.85	159 ± 82	0.82	169 ± 55	0.96
Epi- <i>T</i> _{SID} (HB)	883 ± 604	<0.001	379 ± 210	<0.01	221 ± 65	<0.001
Epi- <i>T</i> _n (HB)	3,437 ± 2,365	<0.001	1,455 ± 755	<0.01	913 ± 267	<0.001

* Ty-LGE vs ATy-LGE; ** ATy-LGE vs healthy controls; *** Ty-LGE vs healthy controls

Ty-LGE typical LGE pattern; *ATy-LGE* non typical pattern or absence of LGE; *bpm* beats per minutes, *a.u.* Arbitrary unit of signal intensity, *HB* heartbeat, *C*_{sm} average signal intensity of skeletal muscle, *S*₀ y-intercept of signal intensity, *T*_{SID} time of signal intensity decay, *T*_n time of complete myocardial signal intensity decay

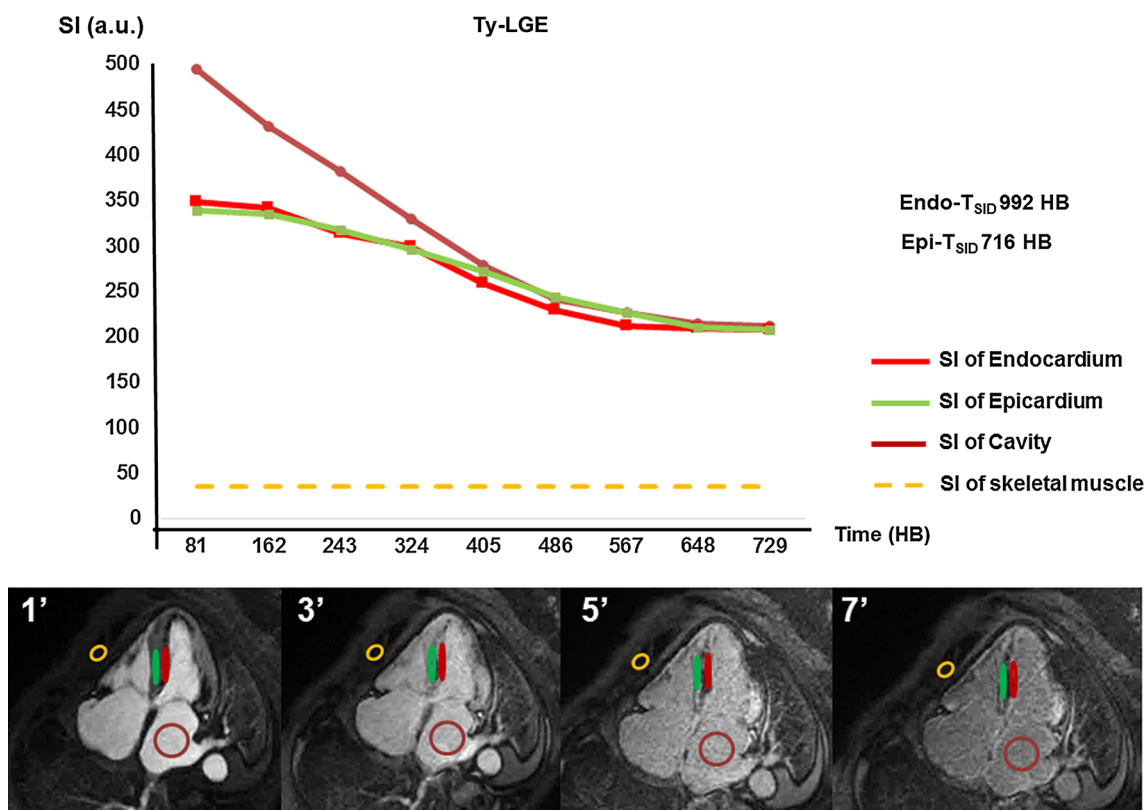


Fig. 2 Signal Intensity Decay (SID) in a CA patient of Ty-LGE group: in the SI/time curves a slow decay of signal measured in endocardial and epicardial ROI is showed. The signal from these

ROIs is still higher than signal of skeletal muscle after 8 min following injection of gadolinium. *CA* cardiac amyloidosis; *Ty-LGE*: typical LGE pattern

No significant association between eGFR and all SID parameters was observed.

ECV measurement was performed in 20 patients in Ty-LGE group and 10 with ATy-LGE and in all the controls. The average ECV was higher in Ty-LGE than in controls (0.36 ± 0.08 vs 0.26 ± 0.03 , $p < 0.001$). ECV was not significantly different in ATy-LGE (0.29 ± 0.09 , $p = 0.16$) than controls.

As evidenced in Fig. 5, a direct relation was found between ECV and Endo-*T*_{SID} (r 0.72, 95 % CI 0.37–0.89, $p < 0.001$) in CA patients. At ROC curve analysis ECV with a threshold of >0.3 had 79 % sensitivity and 93 % specificity to distinguish between Ty-LGE and controls (AUC 0.87). Yet, ECV with a the same threshold had 65 % sensitivity and 93 % specificity to distinguish between CA patients and controls (AUC 0.73). For comparison Endo-

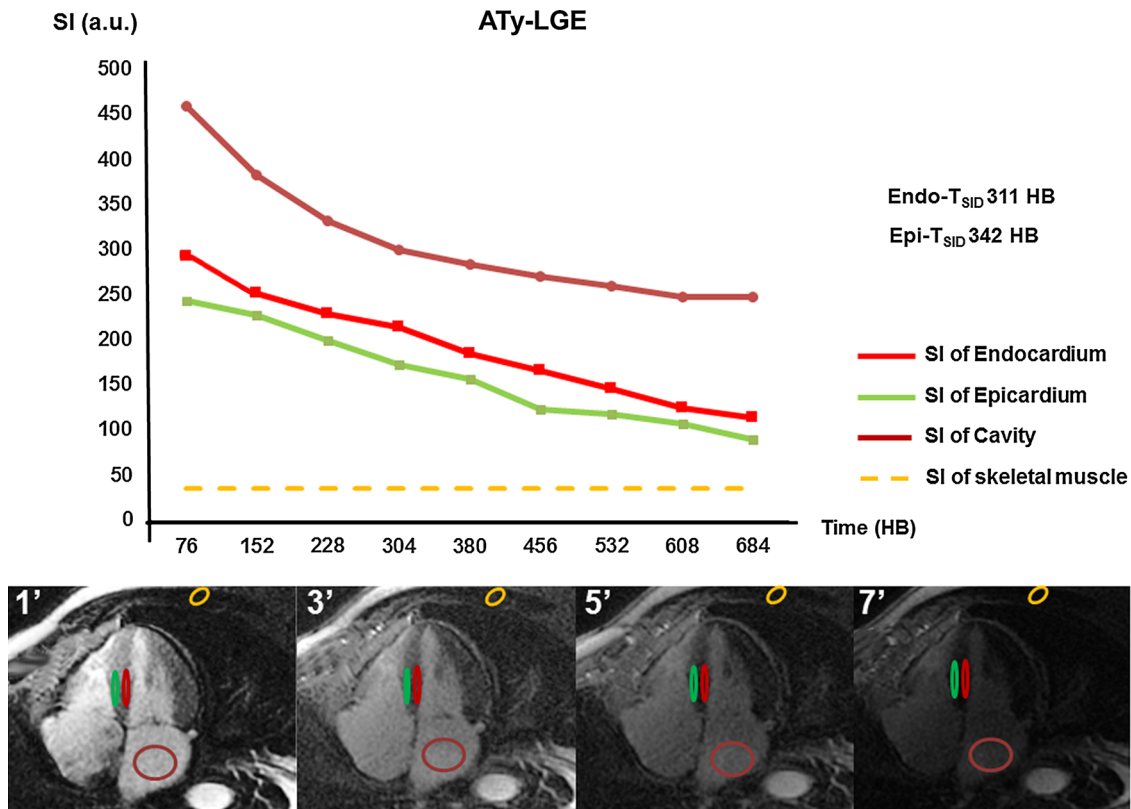
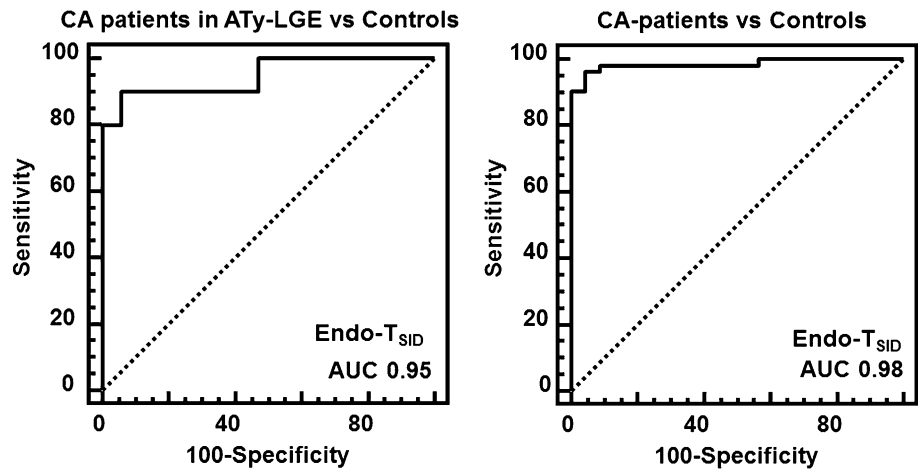


Fig. 3 Signal Intensity Decay (SID) in a CA patient of ATy-LGE group. Also in ATy-LGE group signal decay of endocardial and epicardial is slower than in controls. CA cardiac amyloidosis, ATy-LGE non typical pattern or absence of LGE

Fig. 4 Receiver Operating Characteristic (ROC) curves showing the accuracy of Endo-T_{SID} for the distinction between CA patients of ATy-LGE group and controls (left panel) and between all the CA patients and controls (right panel). CA cardiac amyloidosis, ATy-LGE non typical pattern or absence of LGE



T_{SID} had higher AUC than ECV for the distinction between Ty-LGE and controls ($p < 0.02$) and between Ca patients and controls ($p < 0.01$).

Comparison between LGE and SID for diagnosis of cardiac amyloidosis

Conventional LGE technique and SID method were compared for the diagnosis of CA. As evidenced above, LGE technique

with the typical pattern allowed identification of 42 patients with a definite diagnosis of CA and missed 10 patients with CA having other LGE patterns or absence of myocardial enhancement. No false positive was found. By these results the conventional LGE had 81 % sensitivity and 100 % specificity to detect CA, with 100 % positive predictive value, 73 % negative predictive value, and 87 % diagnostic accuracy.

Considering Endo-T_{SID} range of values in control group (175 ± 47 HB), a threshold of 269 HB, obtained as

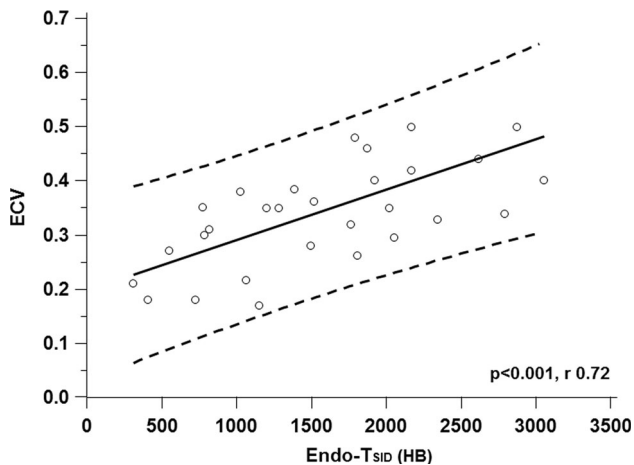


Fig. 5 Scatter diagram showing the relation between extracellular volume (ECV) and the Endo- T_{SID} parameter, expressed in heartbeats (HB)

mean + 2 SD (>95th percentile), was found. The SID method, using the Endo- T_{SID} parameter with a cut-point >269 HB, allowed definite diagnosis of CA in 51 patients, missed the diagnosis in only 1, and returned a false positive diagnosis in 2 cases, with a 98 % sensitivity, and 93 % specificity, 96 % positive predictive value, 96 % negative predictive value, and 96 % diagnostic accuracy.

Discussion

Main results of this study may be summarized as: (1) a slower myocardial SID was demonstrated in CA patients, as compared to controls; (2) the analysis of myocardial SID at subendocardial level after gadolinium injection, a novel CMR technique for CA assessment, shows a higher diagnostic accuracy (96 %) than conventional LGE (87 %), with high specificity, and a higher sensitivity (98 %) than LGE (81 %); (3) a significantly higher myocardial SID value was demonstrated in Ty-LGE, compared to ATy-LGE patients and controls, and in ATy-LGE than in controls; (4) a direct relation was found between ECV and Endo- T_{SID} , but Endo- T_{SID} had higher accuracy or the distinction between CA patients and controls.

An early diagnosis of CA is clinically relevant, because early specific therapy may slow the disease progression, reducing/preventing the intramyocardial deposit of amyloid.

CMR with LGE technique is considered a valid diagnostic tool for the diagnosis CA. The typical findings associated with gadolinium injection in CA is characterized by a diffuse endocardial LGE, with an early darkening of LV cavity and in advanced stages also a diffuse epicardial enhancement [5, 18]. However, these features were described in approximately 70–80 % of patients with CA and is associated to worse prognosis, becoming often

evident only in advanced disease [4, 18]. The 81 % prevalence of the typical LGE pattern in our CA patients was similar to that observed in previous studies [4, 6, 18]. All patients with a typical pattern of LGE had a definite diagnosis of CA and this finding confirmed its optimal specificity. However, in 19 % of CA patients this specific pattern of LGE was absent. Approximately 8 % of CA patients had a different pattern of LGE, usually as focal enhancement in the interventricular septum or in lateral wall; in the remaining 11 %, LGE images showed absence of myocardial enhancement.

In presence of a focal pattern of LGE, alternative diagnosis should be excluded. However, in this study all patients with systemic AL amyloidosis and a focal pattern of LGE had a definite diagnosis of CA. Then, the identification of a typical pattern of LGE may be not sufficient for an early diagnosis of cardiac involvement in patients with systemic AL amyloidosis.

We propose here a new method for the assessment of myocardial SID after the injection of gadolinium-based contrast medium at endocardial and epicardial layers of interventricular septum. In the SID method the inversion time is a constant while the time from gadolinium injection is variable. In both healthy and CA subsets, the signal intensity of skeletal muscle is nulled at the first minute after gadolinium injection, and may be considered as a zero-reference value. In healthy controls, the signal intensity of normal myocardium after gadolinium injection rapidly decreases to the signal of skeletal muscles. On the contrary, the drop of myocardial signal intensity of CA patients is much slower. In fact, dividing Endo- T_n and Epi- T_n (representing the theoretical time in HB to reach the signal of skeletal muscle of endocardium and epicardium) by the HR, we found that the time to completely null myocardial signal may be approximated to 11 min for controls, 19 min for ATy-LGE and 63 min for Ty-LGE. By this, we hypothesized that the evaluation of myocardial SID might be useful for the early detection of CA in a population of patients with systemic AL amyloidosis.

Signal intensity/time curves were generated describing the myocardial SID after gadolinium as a negative exponential function. We introduced Endo- T_{SID} and Epi- T_{SID} as time-parameters describing the curves respectively for the endocardial and epicardial ROIs. We found that both Endo- T_{SID} and Epi- T_{SID} were significantly higher in Ty-LGE than ATy-LGE patients and controls. Moreover, these parameters were also significantly higher in ATy-LGE than controls. These findings suggest that the myocardial SID is slower, even when the typical pattern of LGE is absent. We defined the Endo- T_{SID} normality threshold as the mean value +2 SD (269 HB) from control group analysis. We found that all patients in Ty-LGE group and 9/10 from the ATy-LGE group showed pathological Endo- T_{SID} values,

i.e. >269 HB. The SID method final sensitivity and specificity for the diagnosis of CA were 98 and 93 % respectively (96 % diagnostic accuracy) demonstrating its superiority in comparison with the conventional LGE technique. These results may be explained considering that the velocity of myocardial SID is dependent on the extracellular volume: if amyloid deposit increases the extracellular volume, the SID is slower, and both the Endo- T_{SID} and Epi- T_{SID} are longer. Hence, the measurement of myocardial SID may be considered as an indirect method to assess the myocardial extracellular volume.

Other techniques as T1 mapping and the measurement of the myocardial EVC are currently under evaluation for the diagnosis of CA in patients without the typical LGE pattern [7–11], while their diagnostic accuracy has never been tested against LGE technique. The measurement of the ECV is based on the quantitative evaluation of intramyocardial T1 changes after gadolinium injection. The measurement of myocardial T1 is usually performed by the acquisition of a T1-weighted image set, increasing progressively the inversion time. Then, T1 is measured by the analysis of the Signal Intensity/inversion time curve. This technique implies the use of a dedicated pulse sequence (i.e. ShMOLLI pulse sequence) which currently are not available for all the clinical CMR machines and requires sophisticated post-processing software and multiple mathematical models to obtain myocardial T1 estimation and to evaluate the intramyocardial extracellular volume [19].

However, compared to the direct measurement of the ECV by T1 mapping, the SID method has some advantages. First, the use of conventional LGE images allows the immediate application of this method in all the clinical available CMR machines. Second, the time of acquisition for this method is very short, because it is obtained in the first 8 min after gadolinium injection whereas T1 mapping needs acquisition before contrast and at 5, 10 and 20 min after gadolinium injection. Third, the post-processing is fast and feasible, because the only requirement is the measurement of signal intensity of ROIs placed in the interventricular septum. Results of the current study demonstrated a direct relation between ECV and Endo- T_{SID} but also that this latter parameter had higher accuracy to distinguish CA patients and controls.

In the current study we demonstrated that Endo- T_{SID} may be valid a parameter of SID for the diagnosis of CA, in agreement with previous evidenced showing that the usual pattern of amyloid protein deposition in the myocardium is predominantly subendocardial with variable transmural extension. Previous studies evaluated the T1 of both subendocardial and subepicardial layers and demonstrated that the difference between subepicardial (low amyloid, low gadolinium, high T1) and subendocardial T1 (higher amyloid, higher gadolinium, lower T1) is usually high [4].

Maceira et al. [20] also demonstrated that the 2 min post-gadolinium intramyocardial T1 difference between subepicardium and subendocardium predicting mortality with 85 % accuracy at a threshold value of 23 ms. However, in advanced stages, with greater myocardial amyloid deposition, including the subepicardium, the transmural difference in amyloid diminishes, decreasing the intramural T1 gradient. In these circumstances, the sub-epicardial T1 may be important for prognostic stratification. Endo- T_{SID} and Epi- T_{SID} may act as sub-endocardial and sub-epicardial T1, however, the evaluation of prognostic role of SID parameters was beyond the aim of the current study and future long-term prospective study are needed to assess this point.

Interestingly, in this study patients with Ty-LGE had higher wall thickness, higher LV mass index with lower end-diastolic volume index than patients with Aty-LGE. Yet, E/A ratio was higher in patients with Ty-LGE than in Aty-LGE suggesting a more advanced stage of diastolic dysfunction. Taken together these findings may confirm the hypothesis that Ty-LGE is associated to a worse presentation of CA, with higher degree of hypertrophy and ventricular involvement. Future studies are needed to explain whether patient with Aty-LGE may progress to Ty-LGE or be only associated to a less severe cardiac involvement.

In this study we evaluated the SID technique for the diagnosis of CA but this technique may be also used for the differential diagnosis between CA and other cardiomyopathies. Further studies will be needed to validate SID as method for differential diagnosis in LV hypertrophy.

Some study limitations need to be reported. The diagnosis of CA was obtained by guidelines criteria, and endomyocardial biopsy was performed in a minority of patients presenting with no echocardiographic and electrocardiographic criteria [2]. However, endomyocardial biopsy is an invasive procedure and is associated to a significant percentage of complications. Moreover, amyloid deposit may be not uniformly distributed predisposing to biopsy sampling errors. In our population, endomyocardial biopsy was performed only in patients without a definite diagnosis by echocardiographic and electrocardiographic criteria for CA. Yet, different hemodynamic conditions may alter the velocity of gadolinium wash-out, making more difficult to compare different patients. However, the time-parameters as Endo- T_{SID} and Epi- T_{SID} were indexed by the heart rate in order to normalize values from different patients. The low SD calculated in the control group may justify this approach. Theoretically, renal function may also influence wash out of gadolinium, but Endo- T_{SID} and Epi- T_{SID} were not significant related to eGFR in this work. An intrinsic SID method limitation, shared with the LGE technique and T1 mapping, is associated with its preclusion to patients with severe CKD

(eGFR < 30 mL/min) in which gadolinium-based contrast agents are contraindicated. In this study we evaluated SID using only one contrast medium (Gd-DTPA). Different contrast media may have slight variation in volume of distribution, wash-out kinetics and effect on T1.

Finally, results of the current study did not permit to obtain data regarding the negative predictive value of SID to exclude CA.

In conclusion, this study demonstrates that in subjects with CA the gadolinium kinetics, assessed by the SID method is slower than in controls. The SID method improves diagnostic accuracy of CMR for CA, in comparison with conventional LGE approach. An early diagnosis of CA may be clinically relevant to set up specific treatments able to counteract further amyloid deposit, and subsequent progression towards ventricular dysfunction and failure. Unfortunately, the design of the current study did not permit to evaluate the effectiveness of SID for the early diagnosis of CA and further clinical studies in larger populations are needed.

Conflict of interest No conflict of interest declared.

References

- Falk RH (2005) Diagnosis and management of the cardiac amyloidosis. *Circulation* 112:2047–2060
- Gertz MA, Comenzo R, Falk RH, Fermand JP, Hazenberg BP, Hawkins PN, Merlini G, Moreau P, Ronco P, Sanchowala V, Sezer O, Solomon A, Gateau G (2005) Definition of organ involvement and treatment response in immunoglobulin light chain amyloidosis (AL): a consensus opinion from the 10th International Symposium on Amyloid and Amyloidosis, Tours, France, 18–22 April 2004. *Am J Hematol* 79:319–328
- Sanchowala V (2006) Light-chain (AL) amyloidosis: diagnosis and treatment. *Clin J Am Soc Nephrol* 1:1331–1341
- Maceira AM, Joshi J, Prasad SK, Moon JC, Perugini E, Harding I, Sheppard MN, Poole-Wilson PA, Hawkins PN, Pennell DJ (2005) Cardiovascular magnetic resonance in cardiac amyloidosis. *Circulation* 111:186–193
- Vogelsberg H, Mahrholdt H, Deluigi CC, Yilmaz A, Kispert EM, Greulich S, Klingel K, Kandolf R, Sechtem U (2008) Cardiovascular magnetic resonance in clinically suspected cardiac amyloidosis: noninvasive imaging compared to endomyocardial biopsy. *J Am Coll Cardiol* 51:1022–1030
- Ruberg FL, Appelbaum E, Davidoff R, Ozonoff A, Kissinger KV, Harrigan C, Skinner M, Manning WJ (2009) Diagnostic and prognostic utility of cardiovascular magnetic resonance imaging in light-chain cardiac amyloidosis. *Am J Cardiol* 103:544–549
- Sharma P, Socolow J, Patel S, Pettigrew RI, Oshinski JN (2006) Effect of Gd-DTPA-BMA on blood and myocardial T1 at 1.5T and 3T in humans. *J Magn Reson Imaging* 23:323–330
- Iles L, Pfluger H, Phrommintikul A, Cherayath J, Aksit P, Gupta SN, Kaye DM, Taylor AJ (2008) Evaluation of diffuse myocardial fibrosis in heart failure with cardiac magnetic resonance contrast-enhanced T1 mapping. *J Am Coll Cardiol* 52:1574–1580
- Piechnik SK, Ferreira VM, Dall'Armellina E, Cochlin LE, Greiser A, Neubauer S, Robson MD (2010) Shortened Modified Look-Locker Inversion recovery (ShMOLLI) for clinical myocardial T1-mapping at 1.5 and 3 T within a 9 heartbeat breath-hold. *J Cardiovasc Magn Reson* 12:69
- Flett AS, Hayward MP, Ashworth MT, Hansen MS, Taylor AM, Elliott PM, McGregor C, Moon JC (2010) Equilibrium contrast cardiovascular magnetic resonance for the measurement of diffuse myocardial fibrosis: preliminary validation in humans. *Circulation* 122:138–144
- Fontana M, White SK, Banyersad SM, Sado DM, Maestrini V, Flett AS, Piechnik SK, Neubauer S, Roberts N, Moon JC (2012) Comparison of T1 mapping techniques for ECV quantification. Histological validation and reproducibility of ShMOLLI versus multibreath-hold T1 quantification equilibrium contrast CMR. *J Cardiovasc Magn Reson* 14:88
- Milanesi M, Barison A, Positano V, Masci PG, De Marchi D, Marinelli L, Hardy CJ, Foo TK, Landini L, Lombardi M (2013) Modified cine inversion recovery pulse sequence for the quantification of myocardial T1 and gadolinium partition coefficient. *J Magn Reson Imaging* 37:109–118
- Sechtem U, Pflugfelder P, Higgins CB (1987) Quantification of cardiac function by conventional and cine magnetic resonance imaging. *Cardiovasc Intervent Radiol* 10:365–373
- Maceira AM, Prasad SK, Khan M, Pennell DJ (2006) Reference right ventricular systolic and diastolic function normalized to age, gender and body surface area from steady-state free precession cardiovascular magnetic resonance. *Eur Heart J* 27:2879–2888
- Maceira AM, Prasad SK, Khan M, Pennell DJ (2006) Normalized left ventricular systolic and diastolic function by steady state free precession cardiovascular magnetic resonance. *J Cardiovasc Magn Reson* 8:417–426
- Aquaro GD, Todiere G, Barison A, Strata E, Marzilli M, Pingitore A, Lombardi M (2011) Myocardial blood flow and fibrosis in hypertrophic cardiomyopathy. *J Card Fail* 17:384–391
- Tofts PS, Brix G, Buckley DL, Evelhoch JL, Henderson E, Knopp MV, Larsson HB, Lee TY, Mayr NA, Parker GJ, Port RE, Taylor J, Weisskoff RM (1999) Estimating kinetic parameters from dynamic contrast-enhanced T1-weighted MRI of a diffusible tracer: standardized quantities and symbols. *J Magn Reson Imaging* 10:223–232
- Perugini E, Rapezzi C, Piva T, Leone O, Bacchi-Reggiani L, Riva L, Salvi F, Lovato L, Branzi A, Fattori R (2006) Non-invasive evaluation of the myocardial substrate of cardiac amyloidosis by gadolinium cardiac magnetic resonance. *Heart* 92:343–349
- Banyersad SM, Sado DM, Flett AS, Gibbs SD, Pinney JH, Maestrini V, Cox AT, Fontana M, Whelan CJ, Wechalekar AD, Hawkins PN, Moon JC (2013) Quantification of myocardial extracellular volume fraction in systemic AL amyloidosis: an equilibrium contrast cardiovascular magnetic resonance study. *Circ Cardiovasc Imaging* 6:34–39
- Maceira AM, Prasad SK, Hawkins PN, Roughton M, Pennell DJ (2008) Cardiovascular magnetic resonance and prognosis in cardiac amyloidosis. *J Cardiovasc Magn Reson* 25:10–54